ACS OMEGA

http://pubs.acs.org/journal/acsodf

Article

Construction of PLGA Porous Microsphere-Based Artificial Pancreatic Islets Assisted by the Cell Centrifugation Perfusion Technique

Chuanjia Guo, Tong Zhang, Jianghai Tang, Chang Gao, Zhimin Zhou,* and Chen Li*

Cite This: *ACS Omega* 2023, 8, 15288−15297

Read Online

ACCESS | Metrics & More | Article Recommendations | Supporting Information

ABSTRACT: Pancreatic islet transplantation is a promising treatment that could potentially reverse diabetes, but its clinical applicability is severely limited by a shortage of organ donors. Various cell loading approaches using polymeric porous microspheres (PMs) have been developed for tissue regeneration; however, PM-based multicellular artificial pancreatic islets' construction has been scarcely reported. In this study, MIN6 (a mouse insulinoma cell line) and MS1 (a mouse pancreatic islet endothelial cell line) cells were seeded into poly(lactic-*co*-glycolic acid) (PLGA) PMs via an upgraded centrifugation-based cell perfusion seeding technique invented and patented by our group. Cell morphology, distribution, viability, migration, and proliferation were all evaluated. Results from glucose-stimulated insulin secretion (GSIS) assay and RNA-seq analysis suggested that MIN6 and MS1-loaded PLGA PMs exhibited better glucose responsiveness, which is partly attributable to vascular formation during PM-dependent islet construction. The present study suggests that the PLGA PM-based artificial pancreatic islets may provide an alternative strategy for the potential treatment of diabetes in the future.

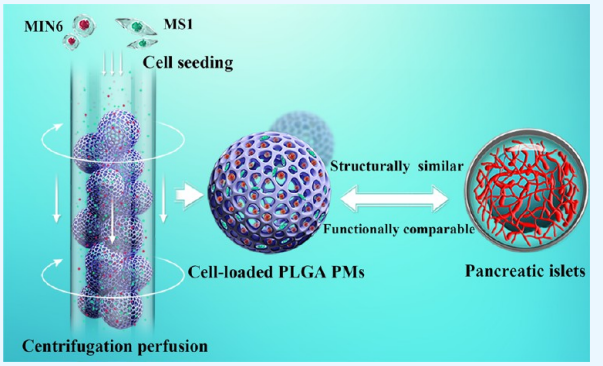

1. INTRODUCTION

Diabetes is a chronic disorder with major global implication. As people with pre-existing medical conditions, diabetic individuals may experience longer and sometimes more difficult recovery due to fluctuations in blood glucose concentrations and the presence of other diabetes-related complications.[1,2] Insulin replacement therapy and antidiabetic agents are currently most commonly prescribed for blood glucose management. Although some major achievements have been made to improve patient compliance and quality of life with fewer occurrences of adverse events such as hypoglycemia, an effective way to reverse diabetes remains to be desired.[3−5]

Pancreatic islet transplantation or islet β-cell replacement therapy has been considered one of the most promising antidiabetic approaches, offering the possibility for complete diabetes recovery.[6] However, the clinical application of islet transplantation is still limited due to the shortage of organ donors and other challenges. In recent years, human and rodent studies have reported the successful generation of functional islets or islet organoids with insulin secretory capacity in response to glucose stimulation from embryonic stem cells, pluripotent stem cells, or dissociated islet cells.[7−9] Meanwhile, approaches that could better accommodate the pancreatic islets during transplantation, such as implementing bioscaffold or islet encapsulation, have been reported.[10,11] However, more efforts are required to validate protocol reproducibility and improve islet cell viability and stability as well as post-transplantation efficacy.

In recent years, the design and implementation of biopolymer-based microcarriers have contributed to the development of advanced tissue models used for pharmacological and pathological research purposes such as drug screening and tissue engineering.[12] By mimicking a structure-specific extracellular matrix (ECM), biopolymer-based microcarriers could provide unique microenvironments that are distinct from the typical two-dimensional (2D) cell culture condition, resulting in increased cellular activity even to the levels observed in vivo.[12,13] Among the numerous biopolymer-based microcarriers, porous microspheres (PMs) have attracted extensive interest in cell-based therapy and drug delivery because of the reported high efficiency in cell/drug loading, cell retention following implantation, and open surgery-free clinical safety.[13−16] Tunable porosity, tailored mechanical strength, and comparatively easy fabrication methods also made using PMs a popular choice for bottom-up tissue

Received: January 20, 2023
Accepted: April 6, 2023
Published: April 19, 2023

Scheme 1. Schematic Illustration of Steps for Artificial Pancreatic Islet Construction by Preparing the MIN6 + MS1 Cell-Loaded PLGA PMs via the Centrifugation Perfusion Cell Seeding Technique

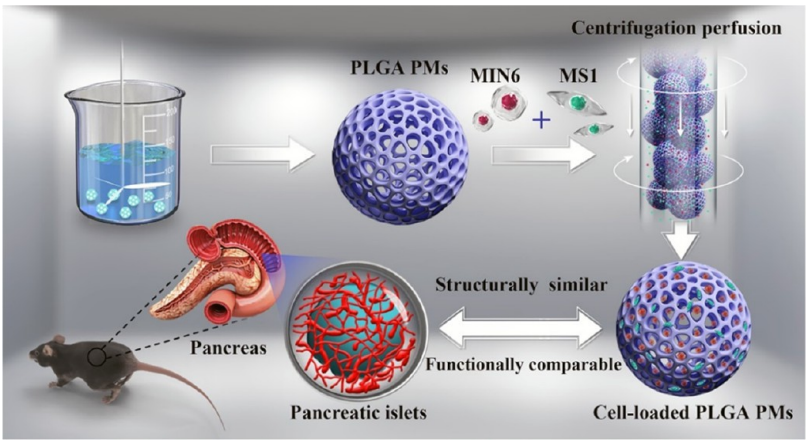

engineering approaches, such as in the design and implementation of microparticle-reinforced composite scaffolds.[17−19] Notably, previous studies have suggested the potential of PMs in stem cell or tissue-specific cell packing during cell therapies, reporting better outcomes over nonporous microspheres and unassisted cell implantation.[12,20] Indeed, excellent cell loading ability has been observed of the PMs either as injectable modularized units or PM-constituted scaffold-supported microtissues.[21,22] However, construction efficiency remains limited regarding organoids, especially vascularized organoids, that require the input of multiple cell types. Various approaches have been proposed and demonstrated, for example, separate seeding of human bone marrow stromal cells (hBMSCs) and human umbilical vein endothelial cells (HUVECs) into cryogel microspheres to construct PM-composed macroscaffolds for bone regeneration.[23] On the other hand, respective modular microtissues were also reported to be designed for muscle regeneration through the injection of composite microtissues harboring C2C12-laden PLGA PMs and HUVEC-laden microrods.[24] Both strategies require further investigation to improve cell seeding efficiency while reducing protocol complexity. As a result, developing an easy and cost-effective way for PM-dependent multicellular organoid construction is both worthwhile and valuable.

In fact, to improve cell adhesion, migration, and infiltration for better cell seeding efficiency, approaches such as surface modification, topological structure optimization, and bioactive molecule incorporation have been employed in scaffold design.[13,25,26] On the other hand, various cell seeding techniques assisted by external forces including gravity, centrifugation, pressure, magnetic, and other bioreactor-driven forces were developed for high-yield cell usage and initial cell distribution in the scaffold.[13,27−30] Centrifugation cell seeding techniques such as centrifugal casting have been developed and applied to improve cell seeding efficiency for bulk scaffold tissue engineering approaches.[30,31] However, the application of centrifugal cell seeding into microcarriers is scarcely explored.

Previously, our group reported the use of PLGA PMs for in vivo delivery of human periodontal ligament stem cells using gravity-forced cell perfusion technology, demonstrating high cell seeding efficiency while retaining cell viability and function.[13] Considering the fact that the pancreatic islets are multicellular micro-organs composed of endocrine cells and extensively vascularized (Scheme 1), for the present study, we focused more on examining the use of the "centrifugation perfusion" seeding technique for multiple cell seeding into PMs for the construction of vascularized and functional "pseudo" pancreatic islets.[32] However, it is worth noting that for multicell PM construction, the lengthy cell seeding process using our previously reported gravity-forced cell perfusion technology is less suitable for simultaneous cell seeding of multiple types of cells, compromising cell viability with an increased risk of contamination.[13] Thus, we also decided to develop an upgraded cell seeding technique applying centrifugation to construct artificial islets.

Herein, in this study, we prepared PLGA PMs as microcarriers by the double emulsion-solvent evaporation technique.[13] Subsequently, the pancreatic MIN6 β-cell line and the islet endothelial cell line MS1 were seeded into as-prepared PLGA PMs with our invented centrifugation perfusion technique for artificial islet construction (Scheme 1). Cell viability, proliferation, and function, i.e., glucose-stimulated insulin secretion and RNA-seq analysis of these PLGA PM-reconstructed artificial "islets", were evaluated.

2. MATERIALS AND METHODS

2.1. Materials. Poly(lactic-*co*-glycolic acid) (PLGA, M_w: 50,000, 50:50, Daigang Biomaterial, Jinan, China), poly(vinyl alcohol) (PVA, degree of polymerization 500, degree of hydrolysis 88%, Sinopec Sichuan Vinylon Works, China), ammonium bicarbonate (Adamas-β, Shanghai, China), dichloromethane (DCM), and sodium hydroxide (NaOH) were obtained from Tianjin Feng-Chuan Chemical Reagent Co., Ltd. (Tianjin, China). Further, 0.25% trypsin−ethylenediaminetetraacetic acid (EDTA), RPMI-1640 medium, Dulbecco's modified Eagle medium (DMEM), and fetal bovine serum (FBS) was purchased from Gibco BRL (Rockville). A 10% normal goat serum-blocking solution and fluorescent carbocyanine dyes DiI (red) and DiO (green) were purchased from Beyotime Biotechnology (Shanghai, China). Bovine serum albumin (BSA), a 4% paraformaldehyde solution (PFA), collagenase V, β-mercaptoethanol, D-glucose, rhodamine-phalloidin solution, and a 4′,6-diamidino-2-phenylindole (DAPI) solution were supplied by Solarbio Technology Co., Ltd. (Beijing, China). A CCK-8 solution and a Hoechst 33258 solution were purchased from Dojindo Laboratories (Kumamoto, Japan).

2.2. Preparation of PLGA PMs. PLGA PMs were prepared by a $W_1/O/W_2$ double emulsion method based on our previously published method.[13] In brief, 2.5 mL of a 1% (w/v

https://doi.org/10.1021/acsomega.3c00424
ACS Omega 2023, 8, 15288−15297

%) NH_4HCO_3 solution (W_1) was added dropwise into the PLGA solution (O, 200 mg of PLGA dissolved in 8 mL of DCM) with a high-speed homogenization speed (3600 rpm) for 2 min. Subsequently, the resulting primary emulsion was immediately poured into 200 mL of a 0.1% (w/v %) PVA aqueous solution (W_2) and stirred for 4 h. The DCM was removed and the PLGA PMs were subjected to hydrolysis with 25 mL of a 0.1 mol/L NaOH aqueous solution for 5 min before being rinsed three times with distilled water. Finally, the aqueous PLGA PM suspension was stored at 4 °C after Co^{60} irradiation sterilization prior to experimental use.

2.3. Physical Characterizations. For morphology investigation of the whole and sectioned PLGA PMs, the diluted suspension of the aqueous microspheres was dropped on the conductive tape, air-dried, and goad-coated by the ion sputter coater. The acquisition of images was carried out by scanning electron microscopy (SEM, ZEISS, MERLIN Compact) operating at an accelerating voltage of 3 kV. Image J software was used to determine the average diameter and surface pore size of the randomly selected microparticles (n = 100). To observe the internal pore structure, the samples were embedded in an optimum cutting temperature (OCT) compound after dehydration, and the cross sections of samples were acquired by a microtome (Leica, Germany) at −20 °C. The frozen sections were dispersed in a 15 mL centrifuge tube and washed with water three times. Finally, the OCT-removed cross sections were examined by SEM as described before. To evaluate the mechanical properties of the PLGA PMs, the force−distance curves were acquired using nanoindentation technology based on atomic force microscopy (AFM, Asylum Research). The cantilever used was AC160TS-R3 (Olympus) with a silicon probe and the tip radius was 10 nm. Young's modulus was calculated by converting force−distance curves to force−indentation curves and fitting the curves with the Hertz model using Igor software (n = 5).

2.4. Cell Culture Conditions. All of the cells were routinely cultured at 37 °C in a 5% CO_2 incubator with a 1% penicillin−streptomycin solution added to cell-specific growth media.

2.4.1. MIN6 and MS1 Cell Culture. Murine insulinoma MIN6 cells were cultured in an RPMI-1640 medium supplemented with 10% FBS and 50 μM β-mercaptoethanol. MS1 cells were cultured in DMEM plus 5% FBS.

2.4.2. Mouse Pancreatic Islet Isolation and Dissociation. Male C57BL/6J mice were purchased from the Experimental Animal Center of the Institution of Radiation Medicine, Chinese Academy of Medical Sciences (Tianjin, China). All animal operations carried out were authorized by the Animal Ethical and Welfare Committee of the Experimental Animal Center of the Institution of Radiation Medicine, Chinese Academy of Medical Sciences (Tianjin, China). Mouse islet isolation was performed as previously reported.[33] Briefly, mice were sacrificed and the pancreas was perfused with a 2 mg/mL collagenase V solution and allowed to digest for 15 min at 37 °C. Purification of pancreatic islets was performed via Histopaque density gradients. The isolated mouse islets were washed and maintained in an RPMI-1640 medium supplemented with 10% FBS under cell culture conditions.

2.5. Cell Loading into the PLGA PMs via the Centrifugation Perfusion Technique. For cell seeding using the centrifugation perfusion technique (pending China patent of No. 202210974999.4. of our group), 15 μL of PBS containing the PLGA PMs was preloaded into the centrifuge tube and rinsed three times by DMEM, and then the cell suspension (4×10^6 cells/mL) was added and thoroughly mixed with the PMs by constant gentle pipetting. The cell/PM suspension was then centrifuged at 1200 rpm for 3 min and the precipitated pellet was resuspended by gentle pipetting several times. This procedure was repeated several times, following which the cell/PM suspension was transferred to a culture dish, and the cell-loaded PMs were collected.

2.6. Cell Distribution, Viability, Proliferation, and Migration in PLGA PMs. For the analysis of cell distribution after cell seeding, the cell suspension was diluted to 10^6 cells/mL and prelabeled with 10 μM fluorescence cell tracker DiI in a 37 °C incubator for 15 min. Then, the cell suspension was washed and seeded as described before. The cross-sectional images of the labeled cells within the PMs were visualized using a confocal laser scanning microscope (CLSM, Carl Zeiss Microscopy GmbH, Germany). For the seeding of both MIN6 and MS1, two fluorescence dyes, DiI and DiO, were used (MIN6 cells in red and MS1 in green).

Cell viability of MS1 and MIN6 cells following the designated culturing period was evaluated via the Calcein-AM/PI double-staining assay by using the Calcein-AM/PI kit according to the manufacturer's instruction (Solarbio, Beijing, China). Fluorescence signals were observed, and the Z-stack images were timely shot by CLSM at 488 nm and 543 nm.

Cell proliferation within the microcarriers following 1, 3, 5, and 7 days of culturing was determined with the CCK-8 Kit (Dojindo, Kumamoto, JP). Procedures were performed as recommended by the manufacturer.

Cell migration was observed and recorded by an optical microscope. The cell attachment of MS1 to PLGA PMs at 3 days was observed and photographed by the CLSM following cell labeling with rhodamine-phalloidin (red) and DAPI (blue). Briefly, the recovered cell-loaded PMs were fixed and then blocked by a 5% BSA solution. The samples were then incubated with the DAPI solution and rhodamine-phalloidin solution while being kept in the dark. Finally, the samples were transferred to a glass-bottom cell culture dish and observed under CLSM.

2.7. Immunohistological Analysis of Insulin Secretion of Cell-Loaded PMs. MIN6 + MS1 cell-loaded PMs cultured for 7 days were first recovered and fixed using 4% PFA for 30 min at room temperature followed by extensive washing. Subsequently, the samples were immersed in 0.5% Triton X-100/PBS at 4 °C for 15 min and blocked with a 10% normal goat serum-blocking solution (Invitrogen). Insulin was stained by exposure to an anti-insulin primary antibody (1:100 dilution, R&D Systems) at 4 °C overnight, followed by incubation with secondary antibody Alexa Fluor 488 goat anti-rat IgG (H + L) (1:100 dilution, Invitrogen) for 2 h at room temperature. A DAPI mounting medium was used before the samples were observed under CLSM.

2.8. *In Vitro* Glucose-Stimulated Insulin Secretion (GSIS) Assay. Static incubation was carried out with MIN6 cells (20,000 cells per well, 96-well plates), MIN6 + MS1 cells (20,000 cells per well, MIN6: MS1 = 1: 1, 96-well plates), MIN6-loaded PMs (100 PMs), and MIN6 + MS1 cell-loaded PMs (100 PMs). In brief, the samples were handpicked into separate Eppendorf tubes and exposed to a physiological salt solution supplemented with 2 or 20 mmol/L glucose for 30 min at 37 °C.[34] Cells were then kept at 37 °C for 45 min, at the end of which cell supernatants and pellets were stored separately at −80 °C. Insulin levels of supernatants and pellets were quantified by using a mouse insulin ELISA kit (Tongwei Biotechnology,

https://doi.org/10.1021/acsomega.3c00424
ACS Omega 2023, 8, 15288−15297

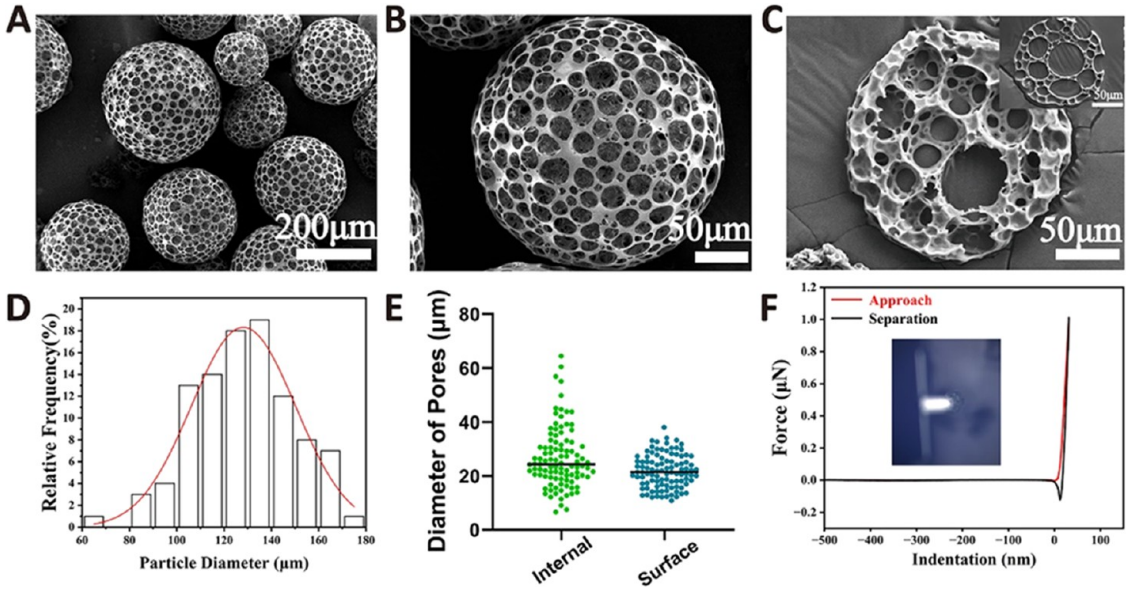

Figure 1. SEM images of the PLGA PMs (A, B) and the inner structure of PLGA PM via the physical section (C). (D) Size distribution of PLGA PMs. (E) Pore diameter distribution of PLGA PMs. (F) Force−indentation curve obtained by AFM.

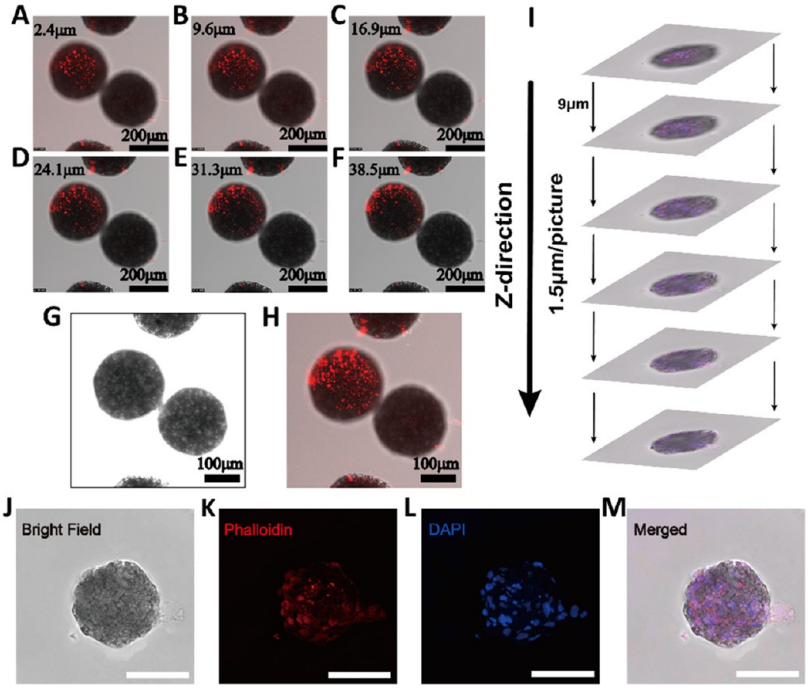

Figure 2. CLSM images of the islet endothelial MS1 cells within the PLGA PMs *in vitro*: (A−F) Z-stack images of MS1 cells 12 h after seeding into the PLGA PMs. MS1 cells stained red. The bright field and merged consecutive images are, respectively, shown in (G) and (H). (I) Scheme for collection of confocal views of MS1-loaded PLGA PMs over 3 days after seeding. (J−M) Fluorescence staining images with an extended depth of the field generated from (I). Nuclei: DAPI, blue; F-actin: phalloidin, red. Scale bars = 100 μm.

Shanghai, China). The capacity of organoids to release insulin in response to glucose was defined as the ratio of insulin produced in high-glucose conditions (20 mmol/L) to insulin secreted in low-glucose conditions (2 mmol/L), known as the glucose stimulation index (GSI).

2.9. RNA-Seq Analysis. The PLGA PM-loaded MIN6 + MS1 cells and 2D-cultured MIN6 + MS1 cells were maintained in culture for 7 days. The total mRNA of PLGA PM-loaded MIN6 + MS1 cells, 2D-cultured MIN6 + MS1 cells, and isolated mouse islets were obtained as previously detailed using a Qiagen RNeasy Plus Mini Kit following the manufacturer's protocol. The mRNA samples were then transferred where quality control and further processing for RNA-seq analysis were performed by APExBIO Technology LLC (Shanghai, China).

2.10. Statistical Analysis. Data are presented as mean ± standard deviation (SD). Statistical significance was analyzed by GraphPad Prism Software (CA), and comparisons between two groups were performed with unpaired Student's *t*-test. Statistical differences between three or more groups were analyzed by one-

https://doi.org/10.1021/acsomega.3c00424
ACS Omega 2023, 8, 15288−15297

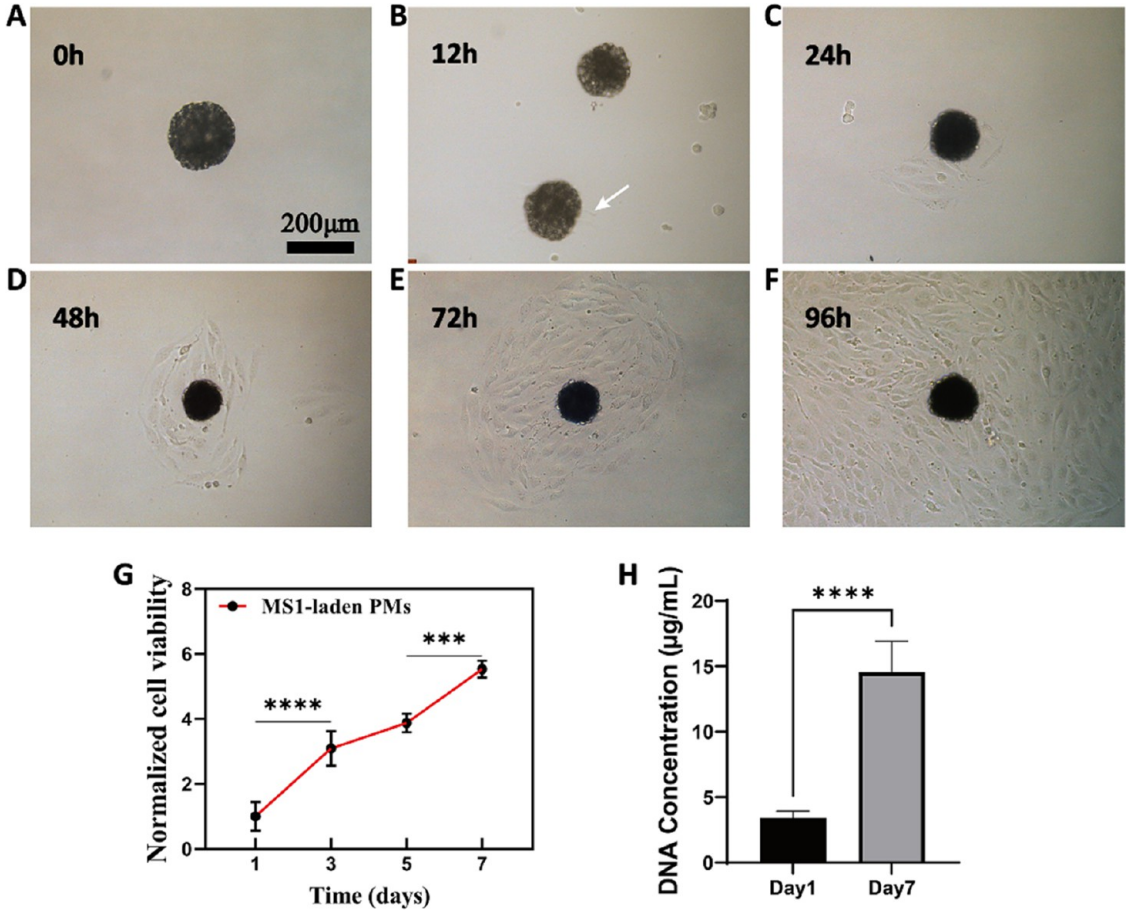

Figure 3. Cell proliferation and migration of the MS1 in the PLGA PMs over 7 days after seeding. (A–F) Optical microscopy images, (G) CCK-8 assay, and (H) DNA content. Data are represented as mean ± SD (n = 4, ***p < 0.001, ****p < 0.0001).

way analysis of variance (ANOVA). Results obtained from GSIS were analyzed using two-way ANOVA.

3. RESULTS AND DISCUSSION

3.1. Physical Characterizations of PLGA PMs. As shown in Figure 1A–C, the PLGA PMs exhibited interconnected interior and exterior pore structures with smooth surfaces. The average diameter of the PLGA PMs ranges from 64.7 to 172.4 μm. (Figure 1D), with a mean average diameter of 128.3 ± 21.7 μm, similar to that of the primary mouse pancreatic islets.[35] Evidently shown by the cross-sectional SEM images of the PLGA PMs following compound dehydration (Figure 1C), the exterior pores are shown as 21.8 ± 6.1 μm in diameter while the interconnected interior pores show average pore diameter of 26.6 ± 11.3 μm (Figure 1E), offering a three-dimensional (3D) microenvironment both suitable for cell infiltration (exterior) and adhesion (interior). In addition to the spatial environment provided by the PLGA PMs, biophysical cues have been lately suggested as another factor that may also impact cell behaviors.[36] Indeed, it has been reported that substrate stiffness, one of the key biophysical factors, participates in mediating cell attachment, migration, spreading, phenotype maintenance, and more. Thus, to further investigate the potential of PLGA PMs in supporting cell growth and function, the mechanical properties of the PLGA PMs were assessed. As shown in Figure 1F, the force–identation curve was generated by AFM and Young's modulus was ca. 1.9 ± 0.2 Gpa. The robust mechanical strength and stiff matrices of the PLGA PMs could be significantly

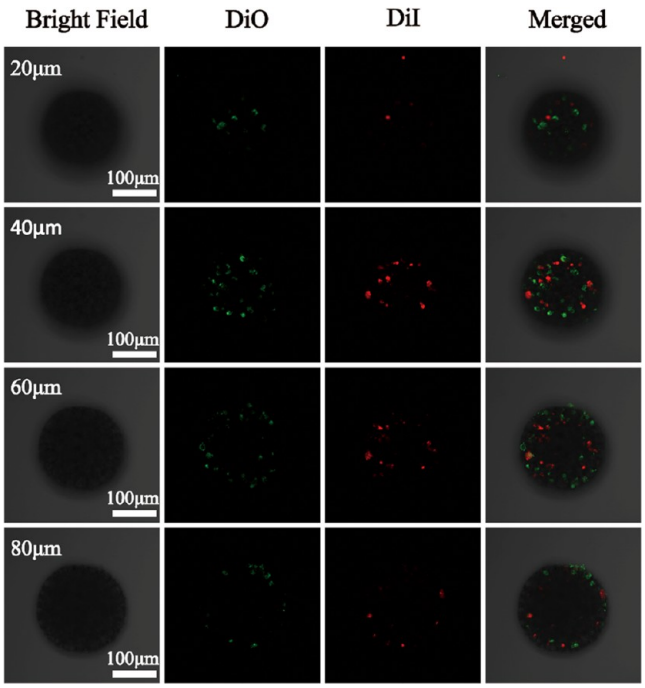

Figure 4. CLSM layer scanning images of MIN6 (red) and MS1 (green) cell-loaded PLGA PMs over 1 day after seeding.

https://doi.org/10.1021/acsomega.3c00424
ACS Omega 2023, 8, 15288–15297

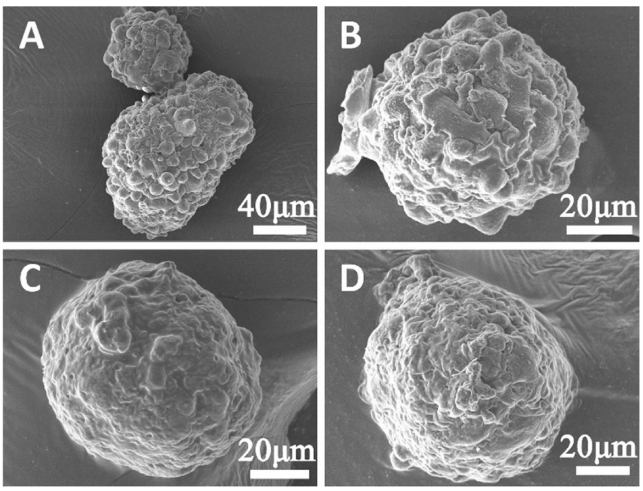

Figure 5. SEM images of MIN6 + MS1 cell-loaded PLGA PMs 7 days after seeding.

impactful in islet cell housing and cell function maintenance. In order to examine the suitability of the PLGA PMs for artificial islet construction, islet cell loading capability was subsequently assessed.

3.2. Optimization of the Cell Seeding Technique and Its Effect on Cell Behavior within the PMs. To investigate the efficiency of the centrifugation perfusion technique and the cell distribution following cell seeding, the cross-sectional images of the prelabeled mouse islet endothelial MS1 cells within the PMs were visualized using CLSM. This is partly because the pancreatic islets are highly vascularized, demanding more than 20% of total pancreatic blood flow while accounting for merely 2% of the entire pancreas mass.[6,32,35] Addition of the MS1 cells would offer vascularization of the PLGA PM-constructed islets and benefit subsequent cell function. Thus, to visualize the distribution of MS1 within PLGA PMs, the MS1 cells were prelabeled with a fluorescence dye, Dil, before the seeding procedure, following which the cell-loaded PLGA PMs were examined by CLSM after being in culture for 12 h. As shown in Figure 2A–H and Supporting Information, Video S1, 12 h after cell seeding, the red fluorescence signals that

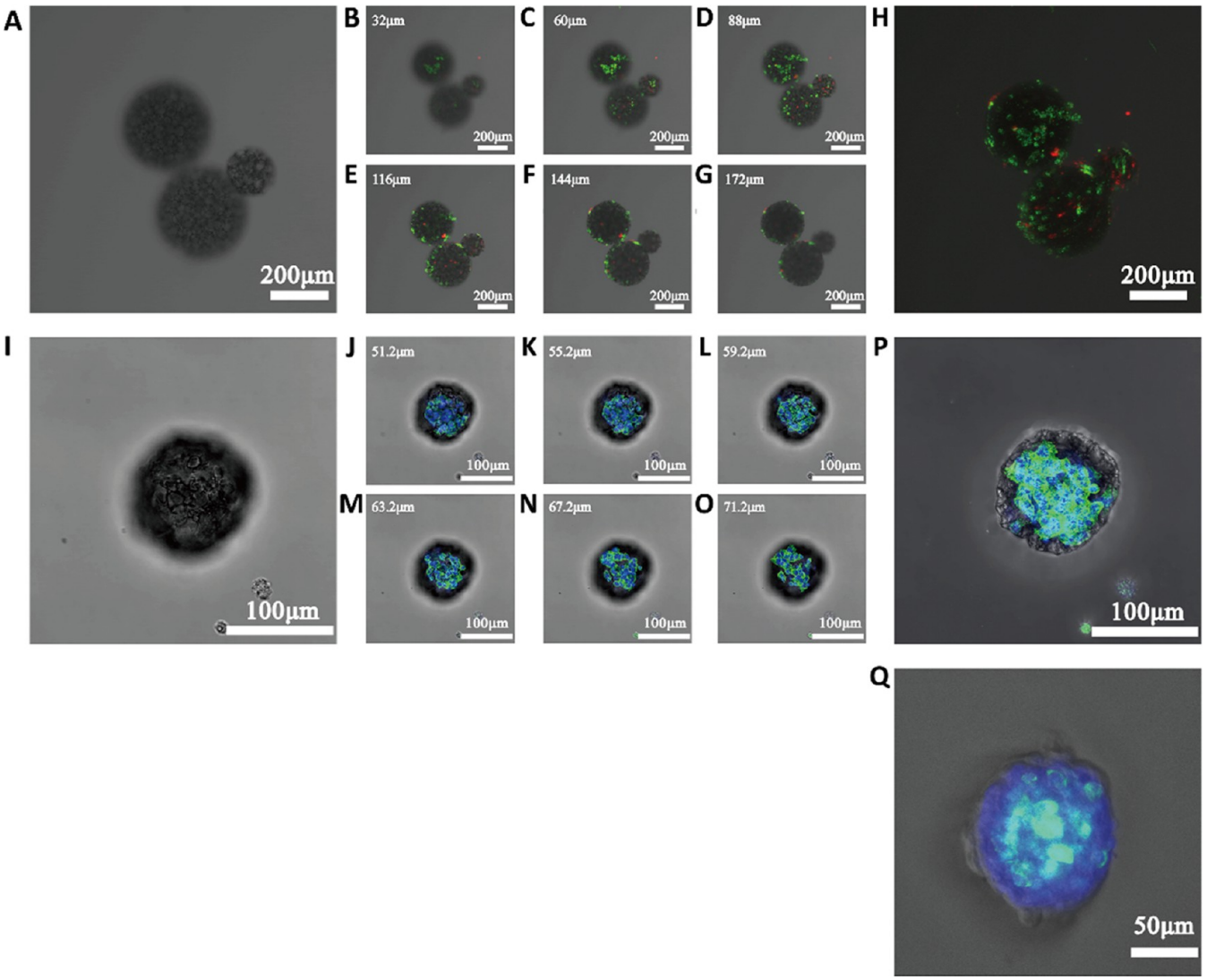

Figure 6. Live/dead cell staining images (A–H) and insulin immunofluorescence staining (I–P) of MS1 and MIN6 within PLGA PMs after 7 days of culture *in vitro*. (Q) Insulin immunostaining of mouse islets.

https://doi.org/10.1021/acsomega.3c00424
ACS Omega 2023, 8, 15288–15297

A

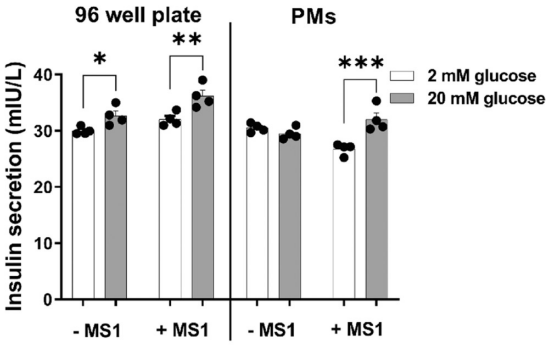

B

	MIN6	MS1 + MIN6	PMs+ MIN6	PMs+ MS1 + MIN6
Glucose stimulation index (GSI)	1.09 ± 0.06	1.13 ± 0.06	0.97 ± 0.03	1.20 ± 0.08

Figure 7. Glucose-stimulated insulin secretion (A) of MIN6 seeded on the 96-well plate and in the PLGA PMs with or without MS1 after 12 h. (B) Glucose stimulated index. Data are represented as mean ± SD (n = 4, *p < 0.05, **p < 0.01, ***p < 0.001).

correspond to Dil-labeled MS1 cells increased significantly as the scanning depth increased toward the core region of the PLGA PMs, implicating excellent cell loading and retention capability.

The morphology of the MS1 cells seeded into the PLGA PMs was further examined by cytoskeleton staining with phalloidin. Thus, MS1 cells were seeded the same way into the PLGA PMs and maintained in culture for 3 days, following which the cells within PLGA PMs were stained with phalloidin (red) and DAPI (blue) (Figure 2I). It can be seen from Figure 2J−M that after 3 days in culture, the MS1 cells were evenly distributed within the PLGA PMs. Supporting Information, Video S2 shows a consecutive scanning view of the PLGA PMs that had been loaded with MS1 cells and maintained in culture for 3 days. Also shown in the video, ribbon-like red filaments could be observed, likely indicating traces of MS1 cell migration within the PLGA PMs.

Indeed, when individual PLGA PMs were maintained in culture to monitor cell behavior, the PLGA PM-loaded MS1 cells could migrate off the PLGA PMs and adhere to the bottom of the culture plate (Figure 3A−F). We observed anchoring of the cell-loaded PLGA PMs to the bottom of the cell culture plate at 12 h post cell seeding, following which individual MS1 cells started to appear (Figure 3B, white arrow), which was in agreement with the previous literature.[13] The cell viability increased as the culturing time extended (Figure 3G). A similar trend was observed in DNA content measurement (Figure 3H), both of which proved excellent cell viability and proliferation of MS1 cells. Our results demonstrated the applicability of the centrifugation perfusion cell seeding technique. Moreover, they also showed that the PLGA PMs supported the viability and function of the seeded MS1 endothelial cells, implicating the positive potential of the PLGA PMs for loading functional endothelial cells during subsequent islet construction.

3.3. PLGA PMs for the Construction of Artificial Islets Based on MIN6 and MS1 Cells. For PLGA PM-based islet construction, pancreatic islet MIN6 cells and islet endothelial MS1 cells were both used. Indeed, islets are highly specified with the unique ability to produce insulin.[6,32,35] The reason for choosing MIN6 cells was mainly because it secretes insulin in response to a high level of glucose stimulation, and has been commonly used as a cell model for islet β-cell investigation.[37] Moreover, polymerase chain reaction (PCR) results using RNAs extracted from MIN6 cells and mouse islets also showed that, similar to the isolated mouse islets, MIN6 cells express mRNAs of both islet hormones insulin and glucagon, and would therefore be suitable for islet construction (Figure S1A).

Similar to that of PLGA PM-loaded MS1 cells, PLGA PM-housed MIN6 cells also exhibited excellent cell viability and morphology (Figure S1B). Considering the importance of vascularization to the maintenance of the islet cell function and survival, we subsequently examined the capability of PLGA PMs for loading both MIN6 and MS1 cells. The cellular performances of each type of cell were also assessed.

Prior to cell seeding, MS1 and MIN6 cells were separately labeled with DiO (green) and DiI (red), respectively. The MIN6 and MS1 cell suspensions were then mixed with a ratio of 1:1 (MS1:MIN6) for cell seeding and maintained in culture. At day 1, the cell-loaded PLGA PMs were observed, and as shown in Figure 4, fluorescence signals of both red and green increased toward the core region of the PLGA PMs (Figure 4, scanning depth of 40 and 60 μm). As expected, the numbers of both types of cells, shown as corresponding fluorescence signals, were comparatively low toward the exterior of the PLGA PMs. Both MIN6 and MS1 cells were relatively evenly distributed. After 7 day's culturing, scanned electron microscopy observed some clusters of cells (Figure 5), indicating the formation of cell−cell contact within the PLGA PMs.

Similar to results obtained from PLGA PMs loaded with only MS1 cells, cell proliferation as indicated by CCK-8 assay and DNA content could be observed as culturing time prolonged (Figure S2A−H). This is also confirmed by live/dead cell staining of the PLGA PMs loaded with both MIN6 and MS1 cells following 7 days in culture (Figure 6A−H). Indeed, a majority of green fluorescence signals that correspond to living cells, with a few dead cells shown in red, were observable, indicating limited cell loss during PLGA PMs' housing.

Immunofluorescence staining of the PLGA PMs loaded with both MIN6 and MS1 cells was then performed to examine the cellular expression of the islet-specific hormone, insulin. As shown in Figure 6I−P, the z-stack images of PLGA PMs showed evident insulin expression (green) within the core region of the PLGA PMs, corresponding to Figure 6P showing central localization of both MIN6 and MS1 cells following cell seeding. Insulin fluorescence staining of native mouse islets was shown as a positive control (Figure 6Q), demonstrating typical insulin expression within the mouse islet core, indicating a fairly similar structural arrangement of the PLGA PMs to isolated mouse islets.

Pancreatic islets are the only known source of insulin secretion with glucose-stimulated insulin secretion being the most important physiological function that is vital for systemic glucose maintenance of stable glucose levels.[35] As a result, being an indicator of the islet construction outcome, we tested the ability of the PLGA PM islets to secret insulin in response to a glucose challenge. Thus, PLGA PM pseudoislets were exposed to a supraphysiological glucose level of 20 mM (Figure 7A). Cells maintained in 2D-culturing conditions were also run as parallel controls. As expected, for 2D-cultured cells, MIN6 cells responded to a high level of glucose stimulation regardless of the presence of MS1 endothelial cells (Figure 7B). This is likely because for 2D culturing, without cell clustering, access to

https://doi.org/10.1021/acsomega.3c00424
ACS Omega 2023, 8, 15288−15297

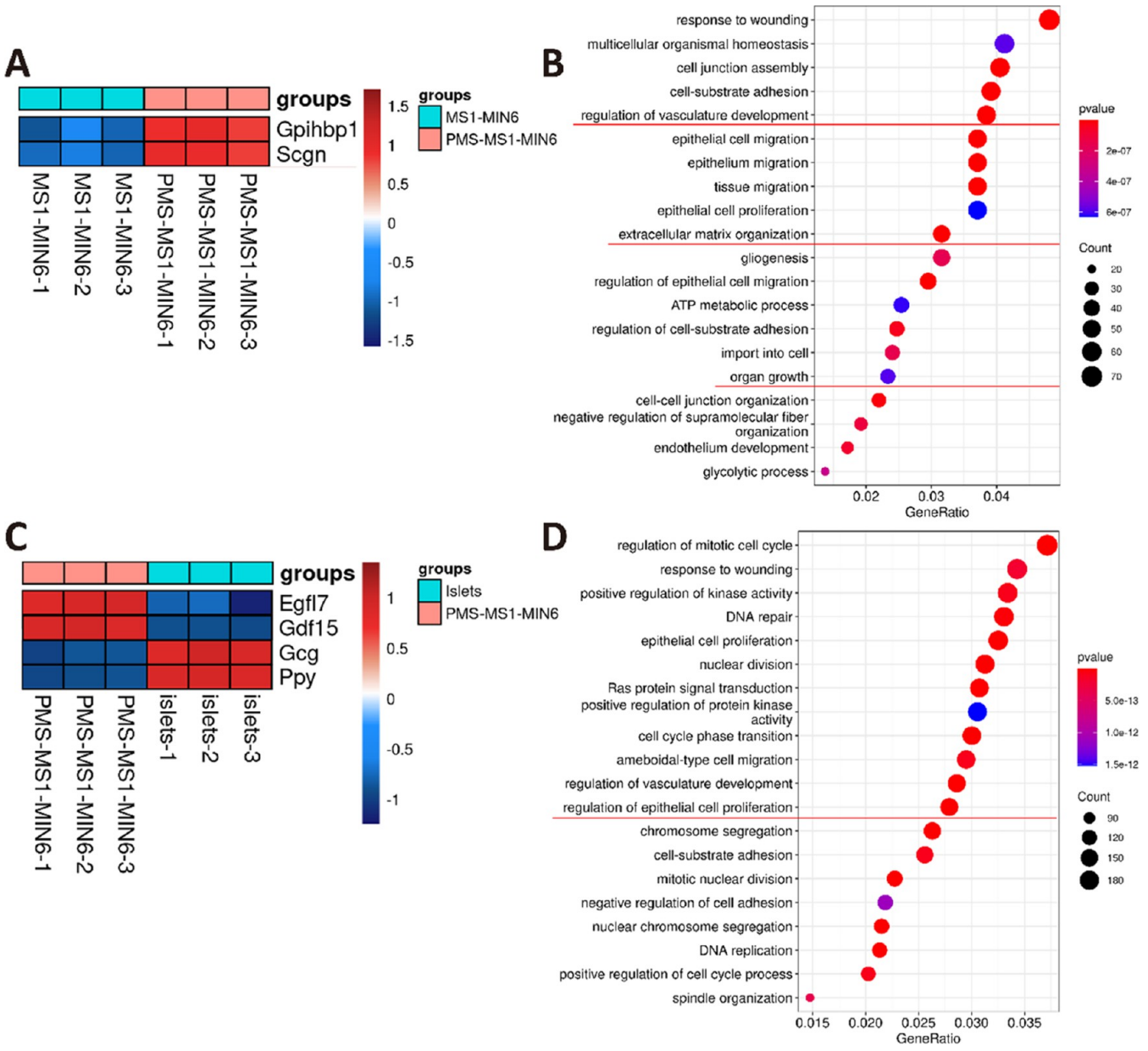

Figure 8. RNA-seq analysis of cells cultured in PLGA PMs. (A) Heatmap of significantly different genes expressed by PLGA PM-loaded MIN6 + MS1 cells vs. 2D-cultured MIN6 + MS1 cells. (B) Categories of top 20 different genes expressed by PLGA PM-loaded MIN6 + MS1 cells and 2D-cultured MIN6 + MS1 cells using enrichment of gene ontology (GO). (C) Heatmap of significantly different genes expressed by PLGA PM-loaded MIN6 + MS1 cells vs. isolated mouse islets. (D) Categories of top 20 different genes expressed by PLGA PM-loaded MIN6 + MS1 cells and isolated mouse islets using enrichment of gene ontology (GO).

oxygen and nutrients is the same for all cells in the culture. In contrast, for PLGA PM islets, insulin secretion in response to a glucose stimulus was only observed from PLGA PMs loaded with MIN6 and MS1 cells, highlighting the importance of vascularization for 3D engineering of functional tissue/organoids.

Indeed, when further analyzed by RNA-seq, the PLGA PM-housed MIN6 and MS1 cells expressed genes that are involved in vascular formation (Figure 8A,B), such as upregulated gpihbp1, encoding a protein expressed by capillary endothelial cells.[38,39] Deficiency of gpihbp1 has been reported to accelerate diabetes-induced atherosclerosis.[40] Secretory element genes that directly modulate insulin secretion, such as the scgn (secretagogin), a calcium-sensing protein that is expressed by islet β-cells, are also upregulated in the PLGA PM-loaded MIN6 and MS1 cells when compared to 2D-cultured MIN6 and MS1 cells, implicating enhanced islet secretory function.[41,42] Moreover, according to GO enrichment results, genes involved in ECM contact and organ formation were also upregulated in PLGA PM-loaded cells (Figure 8B).

When compared to native mouse islets, no compromise in insulin expression was observed from the PLGA PM-loaded MIN6 and MS1 cells (Figure 8C,D). However, as expected of MIN6 cells as an insulin-secreting cell line, lower expression of glucagon (gcg), which is mainly expressed by islet α-cells and pancreatic polypeptide (ppy), which is expressed by islet PP cells was detected for the PLGA PM-loaded MIN6 and MS1 cells when compared to mouse islets. However, similar to when compared to 2D-cultured cells, upregulation of vascular genes was also identified from the PLGA PM-loaded MIN6 and MS1

https://doi.org/10.1021/acsomega.3c00424
ACS Omega 2023, 8, 15288−15297

cells when compared to mouse islets. For example, egfl7, an angiogenic growth factor was upregulated.[43,44] Moreover, other potential antidiabetic candidate genes such as gdf15 (growth differentiation factor 15) were also increased in PLGA PM-loaded MIN6 and MS1 cells, indicating some degree of functional comparability between the PLGA PM pseudoislets and primary mouse islets.

It has long been known that the challenge for 3D tissue regeneration is vascularization since the inner region of the tissue would inevitably be less accessible to oxygen and nutrient supply.[6,24,32] Thus, in line with previous studies, even though PLGA PMs also provided a 3D microenvironment for MIN6 cells as they do for MIN6 + MS1 cells, with minimal compromise to cell viability, cell−cell interaction is vital in maintaining MIN6 cell function as previously reported.[35]

4. CONCLUSIONS

In summary, PLGA PMs that feature the interior and exterior pore structure were prepared using the double emulsion-solvent evaporation method. MIN6 as well as MS1 cells were seeded into PMs for artificial islet construction via the upgraded centrifugation perfusion cell seeding technique, which demonstrated the desirable cell seeding efficiency, viability, and proliferation. The MS1-containing PLGA PM "pseudoislets" were more responsive to the glucose stimulus in terms of insulin secretion, highlighting the importance of functional endothelial cells and vasculature for tissue function. Further RNA-seq analysis also demonstrated upregulated vascular-related genes from the MIN6- and MS1-loaded PLGA PMs, suggesting a positive potential for vascular formation during the PLGA PM-dependent artificial organ construction. Therefore, this facile centrifugation-based cell seeding technique and the PLGA PM-based approach may provide new insights into artificial organ construction in the future.

■ ASSOCIATED CONTENT

Supporting Information

The Supporting Information is available free of charge at https://pubs.acs.org/doi/10.1021/acsomega.3c00424.

Representative images of islet hormone gene expression results obtained from MIN6 cells and mouse islets and of MIN6 cell live/dead staining in the PMs (Figure S1) and results of MIN6 and MS1 cell proliferation in the PLGA PMs over 7 days in culture (Figure S2) (PDF)

Red fluorescence signals that correspond to Dil-labeled MS1 cells increased significantly as the scanning depth increased toward the core region of the PLGA PMs (Video S1) (MP4)

Consecutive scanning view of the PLGA PMs that had been loaded with MS1 cells and maintained in culture for 3 days (Video S2) (MP4)

■ AUTHOR INFORMATION

Corresponding Authors

Zhimin Zhou − *Biomedical Barriers Research Center, Institute of Biomedical Engineering, Chinese Academy of Medical Sciences & Peking Union Medical College, Tianjin Key Laboratory of Biomedical Materials, Tianjin 300192, China*; orcid.org/0000-0003-4832-3530; Email: zhouzm@bme.cams.cn, zhouzhiminf@126.com

Chen Li − *Biomedical Barriers Research Center, Institute of Biomedical Engineering, Chinese Academy of Medical Sciences & Peking Union Medical College, Tianjin Key Laboratory of Biomedical Materials, Tianjin 300192, China*; Email: cli@bme.pumc.edu.cn

Authors

Chuanjia Guo − *Biomedical Barriers Research Center, Institute of Biomedical Engineering, Chinese Academy of Medical Sciences & Peking Union Medical College, Tianjin Key Laboratory of Biomedical Materials, Tianjin 300192, China*

Tong Zhang − *Clinical Laboratory, Tianjin Hospital, Tianjin 300211, China*

Jianghai Tang − *Biomedical Barriers Research Center, Institute of Biomedical Engineering, Chinese Academy of Medical Sciences & Peking Union Medical College, Tianjin Key Laboratory of Biomedical Materials, Tianjin 300192, China*

Chang Gao − *Biomedical Barriers Research Center, Institute of Biomedical Engineering, Chinese Academy of Medical Sciences & Peking Union Medical College, Tianjin Key Laboratory of Biomedical Materials, Tianjin 300192, China*

Complete contact information is available at: https://pubs.acs.org/10.1021/acsomega.3c00424

Notes

The authors declare no competing financial interest.

■ ACKNOWLEDGMENTS

This work was supported by grants from the CAMS Innovation Fund for Medical Sciences (2021-I2M-1-052), the Tianjin Hospital Fund for Science and Technology (Tjyy2109), the Open Fund of Tianjin Key Laboratory of Biomedical Materials (2022BMEKFKT002), the Capital's Funds for Health Improvement and Research (CFH: 2022-2-5072), and the Hygiene and Health Development Scientific Research Fostering Plan of Haidian District Beijing (HP2021-11-80603).

■ REFERENCES

(1) Chamberlain, J. J.; Johnson, E. L.; Leal, S.; Rhinehart, A. S.; Shubrook, J. H.; Peterson, L. Cardiovascular Disease and Risk Management: Review of the American Diabetes Association Standards of Medical Care in Diabetes 2018. *Ann. Intern. Med.* **2018**, *168*, 640−650.

(2) DiMeglio, L. A.; Evans-Molina, C.; Oram, R. A. Type 1 diabetes. *Lancet* **2018**, *391*, 2449−2462.

(3) Sims, E. K.; Carr, A. L. J.; Oram, R. A.; DiMeglio, L. A.; Evans-Molina, C. 100 years of insulin: celebrating the past, present and future of diabetes therapy. *Nat. Med.* **2021**, *27*, 1154−1164.

(4) Beck, R. W.; Bergenstal, R. M.; Laffel, L. M.; Pickup, J. C. Advances in technology for management of type 1 diabetes. *Lancet* **2019**, *394*, 1265−1273.

(5) Vantyghem, M. C.; de Koning, E. J. P.; Pattou, F.; Rickels, M. R. Advances in beta-cell replacement therapy for the treatment of type 1 diabetes. *Lancet* **2019**, *394*, 1274−1285.

(6) Shapiro, A. M. J.; Pokrywczynska, M.; Ricordi, C. Clinical pancreatic islet transplantation. *Nat. Rev. Endocrinol.* **2017**, *13*, 268−277.

(7) Rezania, A.; Bruin, J. E.; Riedel, M. J.; Mojibian, M.; Asadi, A.; Xu, J.; Gauvin, R.; Narayan, K.; Karanu, F.; O'Neil, J. J.; et al. Maturation of human embryonic stem cell-derived pancreatic progenitors into functional islets capable of treating pre-existing diabetes in mice. *Diabetes* **2012**, *61*, 2016−2029.

(8) Lebreton, F.; Lavallard, V.; Bellofatto, K.; Bonnet, R.; Wassmer, C. H.; Perez, L.; Kalandadze, V.; Follenzi, A.; Boulvain, M.; Kerr-Conte, J.; et al. Insulin-producing organoids engineered from islet and amniotic epithelial cells to treat diabetes. *Nat. Commun.* **2019**, *10*, No. 4491.

(9) Du, Y.; Liang, Z.; Wang, S.; Sun, D.; Wang, X.; Liew, S. Y.; Lu, S.; Wu, S.; Jiang, Y.; Wang, Y.; et al. Human pluripotent stem-cell-derived islets ameliorate diabetes in non-human primates. *Nat. Med.* **2022**, *28*, 272−282.
(10) Liang, J. P.; Accolla, R. P.; Soundirarajan, M.; Emerson, A.; Coronel, M. M.; Stabler, C. L. Engineering a macroporous oxygen-generating scaffold for enhancing islet cell transplantation within an extrahepatic site. *Acta Biomater.* **2021**, *130*, 268−280.
(11) Wu, S.; Wang, L.; Fang, Y.; Huang, H.; You, X.; Wu, J. Advances in Encapsulation and Delivery Strategies for Islet Transplantation. *Adv. Healthcare Mater.* **2021**, *10*, No. e2100965.
(12) Huang, L.; Abdalla, A. M. E.; Xiao, L.; Yang, G. Biopolymer-Based Microcarriers for Three-Dimensional Cell Culture and Engineered Tissue Formation. *Int. J. Mol. Sci.* **2020**, *21*, 1895.
(13) Liu, Y.; Zhang, T.; Li, M.; Ouyang, Z.; Gao, F.; Liu, C.; Li, C.; Liu, D.; Zhou, Z. PLGA hybrid porous microspheres as human periodontal ligament stem cell delivery carriers for periodontal regeneration. *Chem. Eng. J.* **2021**, *420*, No. 129703.
(14) Dastidar, D. G.; Saha, S.; Chowdhury, M. Porous microspheres: Synthesis, characterisation and applications in pharmaceutical & medical fields. *Int. J. Pharm.* **2018**, *548*, 34−48.
(15) Kankala, R. K.; Zhao, J.; Liu, C. G.; Song, X. J.; Yang, D. Y.; Zhu, K.; Wang, S. B.; Zhang, Y. S.; Chen, A. Z. Highly Porous Microcarriers for Minimally Invasive In Situ Skeletal Muscle Cell Delivery. *Small* **2019**, *15*, No. e1901397.
(16) Go, G.; Jeong, S. G.; Yoo, A.; Han, J.; Kang, B.; Kim, S.; Nguyen, K. T.; Jin, Z.; Kim, C. S.; Seo, Y. R.; et al. Human adipose-derived mesenchymal stem cell-based medical microrobot system for knee cartilage regeneration in vivo. *Sci. Rob.* **2020**, *5*, No. eaay6626.
(17) Kim, H.; Kim, B. R.; Shin, Y. J.; Cho, S.; Lee, J. Controlled formation of polylysinized inner pores in injectable microspheres of low molecular weight poly(lactide-co-glycolide) designed for efficient loading of therapeutic cells. *Artif. Cells, Nanomed., Biotechnol.* **2018**, *46*, S233−S246.
(18) Yu, H.; You, Z.; Yan, X.; Liu, W.; Nan, Z.; Xing, D.; Huang, C.; Du, Y. TGase-Enhanced Microtissue Assembly in 3D-Printed-Template-Scaffold (3D-MAPS) for Large Tissue Defect Reparation. *Adv. Healthcare Mater.* **2020**, *9*, No. e2000531.
(19) Yang, Y.; Yao, X.; Li, X.; Guo, C.; Li, C.; Liu, L.; Zhou, Z. Non-mulberry silk fiber-based scaffolds reinforced by PLLA porous microspheres for auricular cartilage: An in vitro study. *Int. J. Biol. Macromol.* **2021**, *182*, 1704−1712.
(20) Wei, D. X.; Dao, J. W.; Chen, G. Q. A Micro-Ark for Cells: Highly Open Porous Polyhydroxyalkanoate Microspheres as Injectable Scaffolds for Tissue Regeneration. *Adv. Mater.* **2018**, *30*, No. e1802273.
(21) Tan, Y. J.; Tan, X.; Yeong, W. Y.; Tor, S. B. Hybrid microscaffold-based 3D bioprinting of multi-cellular constructs with high compressive strength: A new biofabrication strategy. *Sci. Rep.* **2016**, *6*, No. 39140.
(22) Paterson, T. E.; Gigliobianco, G.; Sherborne, C.; Green, N. H.; Dugan, J. M.; MacNeil, S.; Reilly, G. C.; Claeyssens, F. Porous microspheres support mesenchymal progenitor cell ingrowth and stimulate angiogenesis. *APL Bioeng.* **2018**, *2*, No. 026103.
(23) Yuan, Z.; Yuan, X.; Zhao, Y.; Cai, Q.; Wang, Y.; Luo, R.; Yu, S.; Wang, Y.; Han, J.; Ge, L.; et al. Injectable GelMA Cryogel Microspheres for Modularized Cell Delivery and Potential Vascularized Bone Regeneration. *Small* **2021**, *17*, No. e2006596.
(24) Wang, Y.; Kankala, R. K.; Cai, Y. Y.; Tang, H. X.; Zhu, K.; Zhang, J. T.; Yang, D. Y.; Wang, S. B.; Zhang, Y. S.; Chen, A. Z. Minimally invasive co-injection of modular micro-muscular and micro-vascular tissues improves in situ skeletal muscle regeneration. *Biomaterials* **2021**, *277*, No. 121072.
(25) Wei, D.; Qiao, R.; Dao, J.; Su, J.; Jiang, C.; Wang, X.; Gao, M.; Zhong, J. Soybean Lecithin-Mediated Nanoporous PLGA Microspheres with Highly Entrapped and Controlled Released BMP-2 as a Stem Cell Platform. *Small* **2018**, *14*, No. e1800063.
(26) Wang, X.; Lin, M.; Kang, Y. Engineering Porous beta-Tricalcium Phosphate (beta-TCP) Scaffolds with Multiple Channels to Promote Cell Migration, Proliferation, and Angiogenesis. *ACS Appl. Mater. Interfaces* **2019**, *11*, 9223−9232.
(27) Liu, Y.; Wu, H.; Jia, Z.; Du, B.; Liu, D.; Zhou, Z. Silk fibroin-modified polylactic acid-glycolic acid copolymer porous microspheres as gingival mesenchymal stem cells delivery carrier. *Chem. J. Chin. Univ.* **2019**, *40*, 2419−2426.
(28) Tavassoli, H.; Alhosseini, S. N.; Tay, A.; Chan, P. P. Y.; Weng Oh, S. K.; Warkiani, M. E. Large-scale production of stem cells utilizing microcarriers: A biomaterials engineering perspective from academic research to commercialized products. *Biomaterials* **2018**, *181*, 333−346.
(29) Villalona, G. A.; Udelsman, B.; Duncan, D. R.; McGillicuddy, E.; Sawh-Martinez, R. F.; Hibino, N.; Painter, C.; Mirensky, T.; Erickson, B.; Shinoka, T.; Breuer, C. K. Cell-seeding techniques in vascular tissue engineering. *Tissue Eng., Part B* **2010**, *16*, 341−350.
(30) Mironov, V.; Kasyanov, V.; Markwald, R. R.; Prestwich, G. D. Bioreactor-free tissue engineering: directed tissue assembly by centrifugal casting. *Expert Opin. Biol. Ther.* **2008**, *8*, 143−152.
(31) Dar, A.; Shachar, M.; Leor, J.; Cohen, S. Optimization of cardiac cell seeding and distribution in 3D porous alginate scaffolds. *Biotechnol. Bioeng.* **2002**, *80*, 305−312.
(32) Dybala, M. P.; Kuznetsov, A.; Motobu, M.; Hendren-Santiago, B. K.; Philipson, L. H.; Chervonsky, A. V.; Hara, M. Integrated Pancreatic Blood Flow: Bidirectional Microcirculation Between Endocrine and Exocrine Pancreas. *Diabetes* **2020**, *69*, 1439−1450.
(33) Zmuda, E. J.; Powell, C. A.; Hai, T. A method for murine islet isolation and subcapsular kidney transplantation. *J. Vis. Exp.* **2011**, *50*, No. e2096.
(34) Gao, S.; Zhang, X.; Qin, Y.; Xu, S.; Zhang, J.; Wang, Z.; Wang, W.; Kong, D.; Li, C. Dual actions of Netrin-1 on islet insulin secretion and immune modulation. *Clin. Sci.* **2016**, *130*, 1901−1911.
(35) Roscioni, S. S.; Migliorini, A.; Gegg, M.; Lickert, H. Impact of islet architecture on beta-cell heterogeneity, plasticity and function. *Nat. Rev. Endocrinol.* **2016**, *12*, 695−709.
(36) Lee, S. S.; Du, X.; Kim, I.; Ferguson, S. J. Scaffolds for bone-tissue engineering. *Matter* **2022**, *5*, 2722−2759.
(37) Miyazaki, J.-I.; Araki, K.; Yamato, E.; Ikegami, H.; Asano, T.; Shibasaki, Y.; Oka, Y.; Yamamura, K.-I. Establishment of a pancreatic β cell line that retains glucose-inducible insulin secretion: special reference to expression of glucose transporter isoforms. *Endocrinology* **1990**, *127*, 126−132.
(38) Fong, L. G.; Young, S. G.; Beigneux, A. P.; Bensadoun, A.; Oberer, M.; Jiang, H.; Ploug, M. GPIHBP1 and Plasma Triglyceride Metabolism. *Trends Endocrinol. Metab.* **2016**, *27*, 455−469.
(39) Young, S. G.; Fong, L. G.; Beigneux, A. P.; Allan, C. M.; He, C.; Jiang, H.; Nakajima, K.; Meiyappan, M.; Birrane, G.; Ploug, M. GPIHBP1 and Lipoprotein Lipase, Partners in Plasma Triglyceride Metabolism. *Cell Metab.* **2019**, *30*, 51−65.
(40) Liu, X.; Li, J.; Liao, J.; Wang, H.; Huang, X.; Dong, Z.; Shen, Q.; Zhang, L.; Wang, Y.; Kong, W.; et al. Gpihbp1 deficiency accelerates atherosclerosis and plaque instability in diabetic Ldlr$^{-/-}$ mice. *Atherosclerosis* **2019**, *282*, 100−109.
(41) Sharma, A. K.; Khandelwal, R.; Sharma, Y. Veiled Potential of Secretagogin in Diabetes: Correlation or Coincidence? *Trends Endocrinol. Metab.* **2019**, *30*, 234−243.
(42) Qin, J.; Liu, Q.; Liu, Z.; Pan, Y. Z.; Sifuentes-Dominguez, L.; Stepien, K. P.; Wang, Y.; Tu, Y.; Tan, S.; Wang, Y.; et al. Structural and mechanistic insights into secretagogin-mediated exocytosis. *Proc. Natl. Acad. Sci. U.S.A.* **2020**, *117*, 6559−6570.
(43) Lau, S. F.; Cao, H.; Fu, A. K. Y.; Ip, N. Y. Single-nucleus transcriptome analysis reveals dysregulation of angiogenic endothelial cells and neuroprotective glia in Alzheimer's disease. *Proc. Natl. Acad. Sci. U.S.A.* **2020**, *117*, 25800−25809.
(44) Usuba, R.; Pauty, J.; Soncin, F.; Matsunaga, Y. T. EGFL7 regulates sprouting angiogenesis and endothelial integrity in a human blood vessel model. *Biomaterials* **2019**, *197*, 305−316.

https://doi.org/10.1021/acsomega.3c00424
ACS Omega 2023, 8, 15288−15297